Defining the Properties of the Nonhelical Tail Domain in Type II Keratin 5: Insight from a Bullous Disease-causing Mutation

Li-Hong Gu and Pierre A. Coulombe

Departments of Biological Chemistry and Dermatology, The Johns Hopkins University School of Medicine, Baltimore, MD 21205

Inherited mutations in the intermediate filament (IF) proteins keratin 5 (K5) or keratin 14 (K14) cause epidermolysis bullosa simplex (EBS), in which basal layer keratinocytes rupture upon trauma to the epidermis. Most mutations are missense alleles affecting amino acids located in the central α-helical rod domain of K5 and K14. Here, we study the properties of an unusual EBS-causing mutation in which a nucleotide deletion (1649delG) alters the last 41 amino acids and adds 35 residues to the C terminus of K5. Relative to wild type, filaments coassembled in vitro from purified K5-1649delG and K14 proteins are shorter and exhibit weak viscoelastic properties when placed under strain. Loss of the C-terminal 41 residues contributes to these alterations. When transfected in cultured epithelial cells, K5-1649delG incorporates into preexisting keratin IFs and also forms multiple small aggregates that often colocalize with hsp70 in the cytoplasm. Aggregation is purely a function of the K5-1649delG tail domain; in contrast, the cloned 109 residue-long tail domain from wild type K5 is distributed throughout the cytoplasm and colocalizes partly with keratin IFs. These data provide a mechanistic basis for the cell fragility seen in individuals bearing the K5-1649delG allele, and point to the role of the C-terminal 41 residues in determining K5's assembly properties.

INTRODUCTION

Intermediate filaments (IFs) are encoded by a large family of genes comprising >67 members in the human and mouse genomes (Coulombe *et al.*, 2001; Hesse *et al.*, 2001). These 10- to 12-nm wide filaments are prominent structural constituents of the cytoplasm and nucleus in multicellular eukaryotes, but they are distinct from F-actin and microtubules in several key respects. Among them is their association with disease. Inherited mutations in IF proteins are associated with nearly 30 human diseases (Omary *et al.*, 2004). These conditions are dominantly inherited with rare exceptions (Fuchs and Cleveland, 1998; Cassidy *et al.*, 2002; Omary *et al.*, 2004), consistent with the complexity of the assembly pathway and of the architecture of mature IF polymers (Herrmann and Aebi, 2004). Cell and tissue fragility underlies lesion pathogenesis in many of these disorders, reflecting the major function of structural scaffolding fulfilled by IFs in both the cytoplasm and nucleus (Omary *et al.*, 2004; Worman and Courvalin, 2004).

Types I and II keratin genes together represent ~75% of IF genes and are specifically expressed in epithelial cells (Coulombe *et al.*, 2001; Hesse *et al.*, 2001). In part because of a strict heteropolymerization requirement at the protein level (Herrmann and Aebi, 2004), type I and type II keratin genes are tightly regulated in a pairwise and differentiation-related manner in epithelial tissues (Moll *et al.*, 1982; O'Guin *et al.*, 1990; Fuchs, 1995). Correlating with frequent exposure to mechanical stress, epithelia lining up the skin and oral mucosa are keratin rich and sensitive to mutations compromising the structural scaffolding function of keratin IFs. Accordingly, a large fraction of the known IF-based disorders affect keratin genes expressed in skin epithelia (Cassidy *et al.*, 2002; Omary *et al.*, 2004). Because of an overlapping distribution of several type I and II keratins in complex epithelia, functional redundancy acts as a powerful modulator of the expressivity of mutant alleles (Herrmann *et al.*, 2003; Coulombe *et al.*, 2004; Wong *et al.*, 2005).

Epidermolysis bullosa simplex (EBS) was the first condition found to be caused by mutations in an IF gene (Coulombe *et al.*, 1991, 2004). In this disorder, the basal layer of epidermis (and, in severe instances, internal stratified epithelia) ruptures readily when the skin is exposed to mechanical rubbing, producing blisters that are painful and debilitating (Fine *et al.*, 1991; Paller, 2004). Whereas the severity of EBS can span a surprisingly wide range, leading to the definition of three major clinical subtypes (Weber–Cockayne, Koebner, and Dowling–Meara; Fine *et al.*, 1991), most cases arise from mutations in the coding sequence of the type II K5 and type I K14, the main keratin pair expressed in basal keratinocytes of the epidermis (O'Guin *et al.*, 1990; Fuchs, 1995). This provided a genetic basis for the anomalies seen in the organization of keratin IFs in basal keratinocytes in EBS patients' skin (Anton-Lamprecht, 1983) and in culture (Kitajima *et al.*, 1989). The ~140 mutations identified in K5 and K14 consist mostly of missense alleles that affect residues located within the central α-helical rod domain (Cassidy *et al.*, 2002), known to play a major role in IF assembly (Herrmann and Aebi, 2004). Characterization of the properties of some of these mutant proteins has helped further our understanding of IF assembly, regulation, and function. Generally, severity of the clinical presentation correlates with the impact exerted by the mutation on the assembly and structure of keratin IFs in vitro and in vivo (Letai *et al.*, 1993; Irvine and McLean, 1999; Porter and Lane, 2003; Omary *et al.*, 2004).

In recent years, the genetic basis of rarer forms of EBS was found to involve a distinct group of target genes, including plectin, integrin β4, and BP180 (Chavanas *et al.*, 1996; Pulkkinen *et al.*, 1996; Smith *et al.*, 1996; Huber *et al.*, 2002; Jonkman *et al.*, 2002; Fontao *et al.*, 2004), or a different type of mutation in the K5 gene. In this latter case, a mutation resulting in a $Pro_{24} \rightarrow Leu$ substitution in the N-terminal head domain of K5 causes EBS with mottled pigmentation (Uttam *et al.*, 1996; Irvine *et al.*, 1997). In addition, a single nucleotide deletion within exon 9 of K5 (1649delG) that results in the frameshift-induced lengthening of K5's C-terminal tail domain was discovered in two independent instances of a form of EBS showing annular migratory circinate erythema (EBS-MCE). In EBS-MCE, a migrating, belt-like erythema with multiple vesicles at the advancing edge of erythema occur on limb extremities and less frequently, on the trunk as well (Gu *et al.*, 2003). Typical of most instances of EBS, however, blistering is restricted to the skin, worsens during the summer during infancy, but gradually subsides with age afterward. Blisters heal normally, with occasional mild hyperpigmentation (Gu *et al.*, 2003). Here, we report on the characterization of the impact of the 1649delG mutation on the assembly properties of K5 in vitro and in transfected cells in culture. Our data provide a mechanistic basis for the cell fragility seen in individuals bearing the K5-1649delG allele and point to the important role of the C-terminal 41 residues in the assembly properties of K5.

MATERIALS AND METHODS

Production, Expression, and Purification of Full-Length Recombinant Proteins

Plasmids pET-K5 and pET-K14 (Coulombe and Fuchs, 1990) were used to obtain purified preparations of human K5 and K14 proteins. Plasmids pET-K5-1649delG and pET-K5CΔ41 were generated using QuikChange site-directed mutagenesis kit (Stratagene, La Jolla, CA). These newly generated constructs were validated by sequencing before use. Bacterially expressed proteins were purified by ion exchange chromatography on Hi-Trap Q and Mono Q columns (Amersham Biosciences, Piscataway, NJ). Heterotypic complexes containing type I and type II keratins in an 1:1 ratio were prepared and purified on Mono Q in Tris-buffered 6.5 M urea (Ma *et al.*, 2001; Yamada *et al.*, 2002). For His-tagged proteins, plasmids pHis-T5 (see below) and pHis-NPT (Bousquet *et al.*, 2001) were expressed into *Escherichia coli* strain BL21 (DE3) followed by fusion protein purification on a nickel column (Novagen, Madison, WI) before cosedimentation assays. Protein purity (>99%) was assessed by SDS-PAGE electrophoresis and Coomassie Blue staining, and protein identity was assessed by Western immunoblotting by using monoclonal antibody (mAb) PCK-26 against K5 (Sigma-Aldrich, St. Louis, MO) and mAb 9E10 against Myc antibody (American Type Culture Collection, Manassas, VA).

Construction of Fusion cDNAs

His Tag Fusion Proteins. The human K5 tail domain coding sequence (residues 482–590; Wilson *et al.*, 1992) was subcloned into a bacterial expression vector, pT7HMT, modified from pT7-6 × His (Bousquet *et al.*, 2001). The sequence of the resulting fusion protein is MGSS<u>HHHHHH</u>SSGLVPRG-SQHMGMEQKLISEEDLNGENLYFQGSTGSM⁴⁸²S, where the His-tag is underlined and S corresponds to residue 482 in K5. pHis-NPT, used as a control, features the neomycin phosphotransferase sequence (GenBank AF335419; M_r 29.2 kDa; Bousquet *et al.*, 2001).

Myc tag Fusion Proteins. The coding sequence of wild-type human K5 (Wilson *et al.*, 1992) and its mutant derivatives K5CΔ111 (Wilson *et al.*, 1992), K5-1649delG, K5CΔ 41, K5E477, and K5D328H (this study) were transferred to vector pcDNA3-Nmyc (Bousquet *et al.*, 2001), which contains a cytomegalovirus promoter and a polyadenylation signal. The strategy used placed the Myc tag (MAEQKLISEEDLLGSM) in-frame at the N terminus of the K5 or mutant coding sequence. A second set of Myc-tagged constructs were engineered in pcDNA3-Nmyc to include the nonhelical tail domains of wild-type K5 and K5-1649delG fused in frame to the N-terminal Myc tag. In this instance, fusion occurs at Ser 482 in K5 (Lersch *et al.*, 1989) and K5-1649delG.

EGFP Fusion Proteins. The full-length wtK5 and K5-1649delG cDNAs were subcloned from pcDNA3-Nmyc into the Bam H1 site of pEGFP-C3 (BD Biosciences Clontech, Palo Alto, CA). In both cases, the keratin open reading frame is fused in frame at the 3' end (C terminus) of the EGFP coding sequences.

All newly generated DNA constructs were validated by sequencing before use.

Filament Assembly and Characterization

Starting from type I-type II heterotypic complexes at 0.5 mg/ml (~10 mM), keratin IFs were reconstituted by serial dialysis by using the following three buffers at room temperature (Ma *et al.*, 2001): 1) 9 M urea, 25 mM Tris-HCl, 10 mM β-mercaptoethanol [β-ME], pH 7., for 4 h; 2) 2 M urea, 5 mM Tris-HCl, 5 mM β-ME, pH 7.4, for 1 h; and 3) 5 mM Tris-HCl, 5 mM β-ME, for >12 h (overnight). The pH of the final buffer was adjusted at 7.4 or 7.0. Filament morphology was examined by negative staining (1% uranyl acetate) and electron microscopy (EM) (CM120; Philips, Kassel, Germany). Sampling was restricted to regions of the EM grid preparations where individual filaments could be seen. Assembly efficiency was determined through high-speed centrifugation (150,000 × *g*, 30 min) in an Airfuge (Beckman Coulter, Fullerton, CA). Supernatant and pellet fractions were analyzed by SDS-PAGE and Coomassie Blue staining. For copelleting assays, 50 μl of assembled keratin (10, 5, and 2.5 μM) and vimentin (10 μM) were mixed with an equal volume of either pHis-T5 (10 μM) or pHis-NPT (10 μM). After 2 h, the mixtures were subjected to high-speed centrifugation and analysis as described above. Human recombinant vimentin was produced and assembled as described previously (Yamada *et al.*, 2003).

Rheological Measurements

Keratin polymers (10 μM; 1.6-ml volume) to be compared were assembled in parallel on the same day and examined by electron microscopy before rheology. Viscoelastic measurements (Ferry, 1980; Coulombe *et al.*, 2000) were obtained using a strain-controlled 50-mm cone-and-plate Rheometrics ARES 100 rheometer (Rheometrics, Piscataway, NJ) as described previously (Bousquet *et al.*, 2001; Ma *et al.*, 2001; Yamada *et al.*, 2002). The linear equilibrium values of the elastic modulus G'(ω) and viscous modulus G''(ω) of the IF polymer suspensions were measured by setting the amplitude of the oscillatory strain at γ = 1% and sweeping from low-to-high frequency ω. The strain-dependent viscoelastic moduli were measured by subjecting the polymers to three cycles of oscillatory deformation of increasing amplitude at 1 rad·s⁻¹; G' and G'' were computed from the maximum magnitude of the measured stress (Ma *et al.*, 2001). Rheological experiments were repeated at least three times by using independent protein preparations, and the findings reported are very consistent between experiments.

Cell Lines, Transfections, and Immunological Reagents

Cell lines were maintained as recommended by their sources: PtK2 (kidney epithelium of the rat kangaroo; American Type Culture Collection) and 308 (mouse epidermal keratinocytes; a gift of Dr. Stuart Yuspa, National Cancer Institute; Strickland *et al.*, 1988). Transient transfections were performed using polyethylenimine (Aldrich Chemical, Milwaukee, WI) as described previously (Boussif *et al.*, 1995; Bousquet *et al.*, 2001) or LipofectAMINE 2000 (Invitrogen, Carlsbad, CA) according to the manufacturer's instruction. At 12, 24, or 48 h posttransfection, cells were fixed with 4.0% paraformaldehyde for 5 min, extracted with 0.1% Triton X-100 in phosphate-buffered saline (PBS) buffer for 5 min., and processed for indirect immunofluorescence. We used rabbit polyclonal antisera against K18 (gift from Dr. E. Fuchs, Howard Hughes Medical Institute, Rockefeller University), K14 (AF64) and K5 (AF138) (Covance, Berkeley, CA), Hsp70 (SPA-812; StressGen, Victoria, Canada), ubiquitin (U5379; Sigma-Aldrich), and α B-crystallin and Hsp27 (gifts from Dr. J. Landry, Centre de Recherche en Cancérologie de l'Université Laval, Quebec; Chavez Zobel *et al.*, 2003); a guinea pig polyclonal antiserum to P62NT (GP62; Research Diagnostics, Flanders, NJ); and mouse monoclonal antibodies against the Myc epitope (clone 9E10; American Type Culture Collection), K8-K18 (L2A1; gift from Dr. M. B. Omary; M. B. Chou *et al.*, 1993), or K14 (LLOO1; gift from Dr. I. Leigh, Centre for Cutaneous Research, Barts and the London School of Medicine and Dentistry; Purkis *et al.*, 1990). Rhodamine- or fluorescein isothiocyanate-conjugated goat anti-mouse, anti-rabbit, or anti-guinea pig secondary antibodies were used (Kirkegaard and Perry Laboratories, Gaithersburg, MD). Samples were analyzed using a Zeiss Axioplan-2 immunofluorescence microscope and a PerkinElmer UltraView confocal microscope.

Keratin Extraction, Coimmunoprecipitation, and Western Blot Analysis

PtK2 cells were harvested 48 h after transfection. Keratin extraction was performed in a three-step procedure: 1) cells were lysed by gentle rotation in low-salt buffer (1× PBS, 1% Triton X-100, 5 mM EDTA, and 0.2 M phenylmethylsulfonyl fluoride [PMSF], supplemented with protease inhibitor cocktails PIC1 and PIC2 [0.1%; Wong and Coulombe, 2003]) at 4°C for 10 min; 2) after centrifugation (16,000 × *g*, 10 min, 4°C), pellets were extracted by gentle

Figure 1. Schematic representation of the mutants tested and expression levels of wild-type and mutant K5 proteins in transiently transfected PtK2 cells. (A) Schematic representation of the tripartite domain structure shared by K5 and all other keratins and intermediate filament proteins. A central α-helical "rod" domain acts as the major determinant of self-assembly and is flanked by nonhelical "head" and "tail" domains at the N and C termini, respectively. The rod domain is segmented into subdomain 1A, 1B, 2A, and 2B separated by three short nonhelical linkers, L1, L12, and L2. The extremities of this rod domain feature 15–20 residue-long regions (dark-shaded boxes) that are highly conserved among all intermediate filaments. For transfection studies only, a Myc or GFP epitope tag was fused in frame to the N terminus of K5. The location and nature of the mutants tested in this study are shown. "ΔX" refers to deletion of X amino acids. The 1649delG mutation induces a frameshift that results in a lengthening of the open reading frame (see black box). Below the full-length K5 diagram is a representation of the Myc-T5 and Myc-T5-1649delG mutant constructs. (B) PtK2 cells (10-cm dishes) were transfected with Myc-tagged K5, wild type and mutant,

as described under *Materials and Methods*. At 48 h posttransfection, cells were harvested, processed for total protein extraction. Proteins were resolved by SDS-PAGE and analyzed by Western blot by using a Myc antibody to detect transfected proteins and a rabbit anti-K18 polyclonal antibody to detect the corresponding endogenous keratin. Bound primary antibodies were detected by enhanced chemiluminescence.
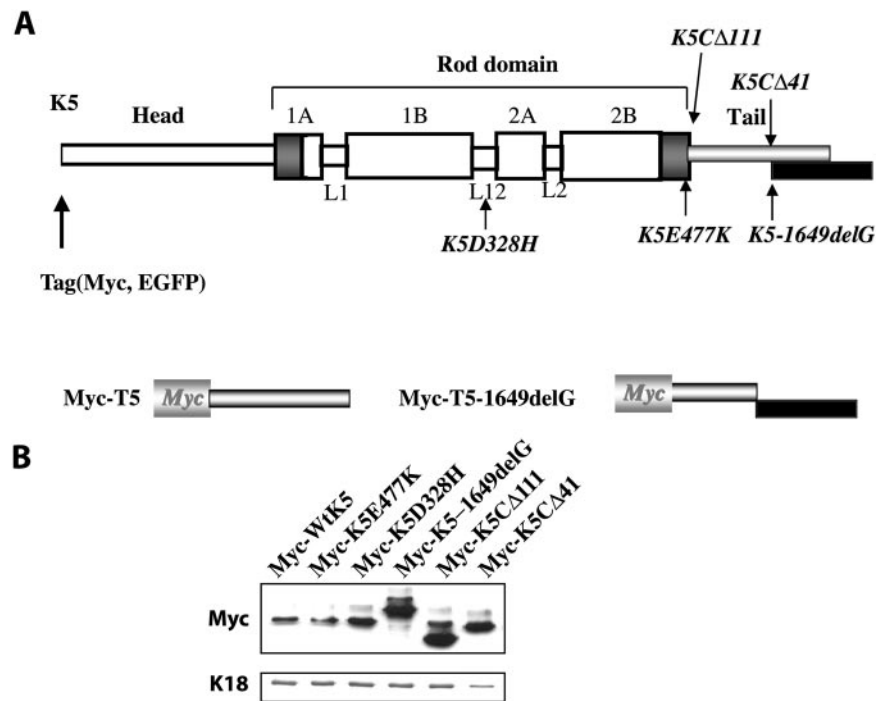
rotation in high-salt buffer (10 mM Tris-HCl, pH 7.6, 140 mM NaCl, 1.5 mM KCl, 5 mM EDTA, 0.5% Triton X-100, 0.2 M PMSF, and 0.1% PIC1 and PIC2) for 30 min at 4°C; and 3) after centrifugation (16,000 × g, 15 min, 4°C), pellets were washed in PBS and dissolved in final buffer (6.5 M urea, 0.2 M PMSF, and 0.1% PIC1 and PIC2). Supernatant and final pellet fractions were then analyzed by SDS-PAGE followed by Western blot analysis. For coimmunoprecipitation, PtK2 cells were lysed by gentle rotation in dithiobis(succinimidyl propionate) (DSP) lysis buffer (2.5 mg/ml DSP, 40 mM HEPES, pH 7.5, 120 mM NaCl, 1 mM EDTA, 1% Triton X-100, 0.2 M PMSF, and 0.1% PIC1 and PIC2) for 30 min at 4°C, followed by addition of 1 M Tris-HCl, pH. 7.5, to end the reaction, and gentle rotation in Empigen BB buffer (1× PBS, 2% EmpBB, 5 mM EDTA, 0.2 M PMSF, and 0.1% PIC1 and PIC2) for 30 min at 4°C. Cell lysates were centrifuged (16,000 × g, 10 min, 4°C), the supernatant transferred to a fresh tube, and K18 antibody (2 μg/ml)-bound protein A-agarose beads (Amersham Biosciences) were added for 2 h at 4°C. Rabbit serum was used as specificity control. The immunoprecipitated samples were washed extensively with lysis buffer, and the pellet was then analyzed by SDS-PAGE and Western immunoblotting by using anti-Myc antibody. Enhanced chemiluminescence (Amersham Biosciences) or alkaline phosphatase (Bio-Rad, Hercules, CA) was used as per the manufacturer's instructions to detect bound primary antibodies on Western blots.

RESULTS

In Vitro Studies

We initially conducted keratin polymerization assays in vitro to determine how the K5-1649delG mutation affects the structural and biophysical properties of keratin filaments. Along with wild-type (wt) K5 and K14, K5-1649delG and K5CΔ41 mutant proteins were overexpressed and purified from *E. coli* and validated using electrophoretic assays (our unpublished data). K5CΔ41 is a C-terminal deletion mutant in which the open reading frame has been interrupted precisely at the location of the frameshift in K5-1649delG (Figure 1A). Purified type I–type II heterotypic keratin complexes were used for dialysis-based assembly. Polymerization efficiency was assessed by centrifugation, and structural features of individual polymers were visualized by negative staining and electron microscopy. Mechanical properties of

the polymers were assessed by rheological assays. None of the mutant tested was impaired in its ability to form urea-stable heterotypic complexes (our unpublished data), as determined by chromatography and chemical cross-linking assays (Wawersik *et al.*, 1997).

When polymerized under standard conditions at pH 7.4, wt K5 and K14 proteins readily form smooth-surfaced filaments (Figure 2A) with very high efficiency (>95%; Figure 2D). These filaments are long (>3 μm), exhibit a diameter of 10.1 ± 0.3 nm (Table 1), and have a natural tendency to form loose aggregates (Figure 2A). In agreement with previous reports (Yamada *et al.*, 2002, 2003), rheological assessment shows that the bulk properties of the wt K5/K14 polymer are typical of those displayed by weak viscoelastic solids, given low values for both phase angle θ and elastic modulus G′ (Table 1). In contrast, polymers assembled from K5-1649delG and K14 are much shorter (Figure 2B), although their diameter (9.6 ± 0.3 nm; Table 1) and polymerization efficiency (Figure 2D) are similar to wt K5/K14. The viscoelastic properties of K5-1649delG/K14 under such conditions are too weak to be reliably measured (Table 1), reflecting the significantly softer and liquid-like character of this sample relative to wt. Similar findings were obtained with the K5CΔ41 mutant (Figure 2, C and D; our unpublished data), implying that the loss of the C-terminal 41 residues in the K5 tail domain contributes significantly to the properties of the K5-1649delG mutant.

We previously showed that assembly of purified keratin proteins in the presence of salt, or alternatively at pH 7.0, fosters the formation of large filament bundles and markedly increases the mechanical resilience of keratin filament assemblies (Ma *et al.*, 2001; Yamada *et al.*, 2002, 2003). Moreover, these modified buffer conditions improve the structural features of filaments assembled from tailless K5 (K5CΔ111) and K14 (Wilson *et al.*, 1992). We find that such is
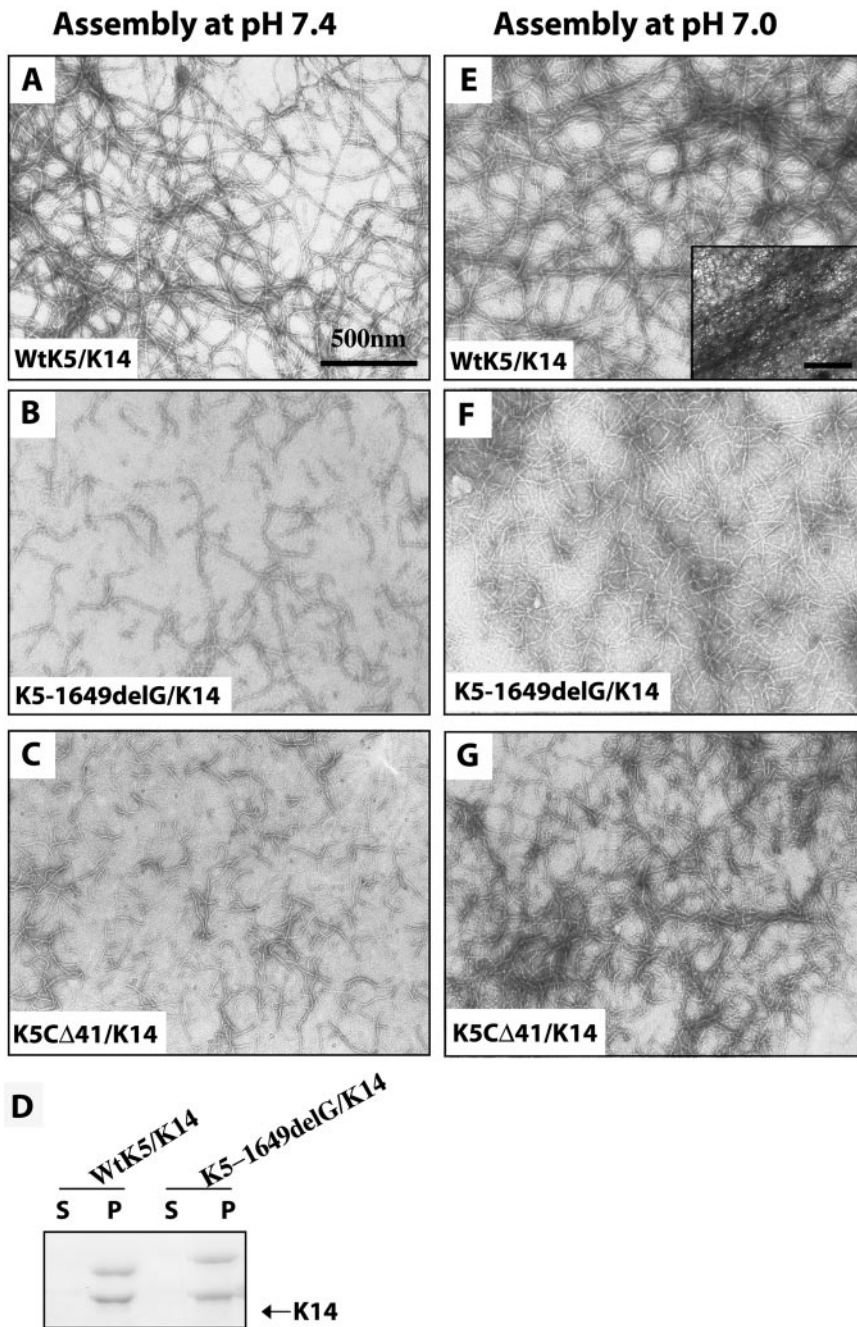
Assembly at pH 7.4   **Assembly at pH 7.0**

Figure 2. Assembly properties of wild-type and mutant K5 proteins. Purified recombinant proteins were copolymerized with partner K14 and assessed by negative staining and electron microscopy (A–C, E–G) and a high-speed filament sedimentation assay (D). (A–D) Polymerization assays were conducted under standard assembly condition at pH 7.4. (E–G) Polymerization was conducted in pH 7.0 buffer, a condition that favors the formation of large keratin filament bundles (see inset, Frame E) (Yamada *et al.*, 2002). The type I–type II composition of polymers is given in the lower left corner of each micrograph. In frame D, s refers to supernatant, and p refers to pellet.

the case as well when copolymerizing either K5-1649delG or K5CΔ41 with K14 at pH 7.0. By negative staining and electron microscopy, both types of filaments seem significantly longer (Figure 2, F and G) compared with those generated at pH 7.4 (Figure 2, B and C), although they do not bundle as effectively as wt K5/K14 (Figure 1E). Rheological testing of K5-1649delG/K14 assembled at pH 7.0 gives rise to an elastic modulus G' which, albeit measurable (Table 1), remain nearly 10-fold lower than that reported for wt K5/K14 under such conditions (Ma *et al.*, 2001; Yamada *et al.*, 2002, 2003). Collectively, these in vitro studies establish that the 1649delG mutation markedly alters the structural features and mechanical properties of K5-containing filaments in a manner that is consistent with the fragilization of basal cells in epidermis in vivo (Gu *et al.*, 2003). These findings also

extend the notion (Wilson *et al.*, 1992) that the tail domain of K5 participates in defining the structural features and properties of keratin filaments reconstituted in vitro.

Transfection Studies Involving Full-Length Proteins

We conducted transient transfection assays coupled with indirect immunofluorescence to compare the behavior of mutant and wild-type K5 when expressed in epithelial cells. Given the subjective nature of this analysis, we added additional K5 mutants (Figure 1A) for reference purpose. K5CΔ111 is a previously characterized deletion mutant in which the entire nonhelical tail domain of K5 has been removed, and which has never been tested through transfection (Wilson *et al.*, 1992). K5-E477K is a missense allele

Table 1. Determination of viscoelastic properties and width of keratin filaments

Sample	pH[a]	Filament width (nm)[b]	Elastic modulus G′ (dynes/cm²)[c]	Phase angle δ (°)[c]
WtK5/K14	7.4	10.1 ± 0.3	5–10	4–8
K5-1649 del G/K14	7.4	9.6 ± 0.3	UN[d]	UN
K5-1649 del G/K14[e]	7.0	10.3 ± 0.2	6–9	5–11

[a] pH refers to the pH of the assembly buffer: pH 7.4 corresponds to the standard condition for polymerizing purified keratins in vitro, whereas pH 7.0 promotes the bundling of K5-K14 filaments (Bousquet *et al.*, 2001; Ma *et al.*, 2001; Yamada *et al.*, 2002, 2003).

[b] Filament width (mean ± SEM) was determined from five filament profiles from each of three micrographs per sample analyzed.

[c] Elastic modulus G and phase angle δ were determined by rheology using conditions of minute deformation (1% strain, and 1 rad/s frequency). The elastic modulus G′ defines the elastic response of a material to a deformation. G′ is directly related to the fraction of the input energy (deformation) that is stored within the material. The phase angle δ, expressed in degrees, corresponds to the delay in the material response due to energy dissipation. The stress response of elastic solids is perfectly in-phase with the imposed strain (deformation), and thus δ = 0°. The stress response of viscous liquids is out of phase with the strain, and δ = 90°. Accordingly, wild-type K5-K14 assemblies behave like weak-viscoelastic solids under standard assembly conditions at pH 7.4. See Coulombe *et al.* (2000) and Yamada *et al.* (2002) for details.

[d] UN, undetectable (below the sensitivity of the instrument).

[e] See Yamada *et al.* (2002, 2003) for corresponding values for WtK5/K14 assembled at pH 7.0. Typically, G′ is >75 dynes/cm², whereas δ is smaller than 6°.

causing a severe (Dowling–Meara) form of EBS disease (Stephens *et al.*, 1997; Pfendner *et al.*, 2003). K5D328H is a missense allele causing a mild (Weber–Cockayne) form of EBS disease (Muller *et al.*, 1998). Immunogenic epitopes specific to K5 are usually located in the distal portion of the tail domain, which is deleted in some of the constructs tested. To circumvent this limitation, we added a Myc epitope tag at the N terminus of the K5 coding sequence (Figure 1A), enabling the detection of all the constructs transfected in PtK2 cells. This cell line, derived from kidney epithelium, features a K8/K18 filament network (Franke *et al.*, 1978) and is well suited for the purpose of assessing mutant keratin properties (Albers and Fuchs, 1987).

Transfection efficiency in PtK2 cells ranged between 17 and 26%, depending upon the DNA construct (Table 2). Expression levels of the transfected proteins also varied, as determined by Western blotting of total PtK2 protein extracts (Figure 1B). These two important elements, transfection efficiency and expression levels, are interdependent and were taken into account when comparing the behavior of mutant and wt K5 proteins. Next, the distribution of mutant proteins and status of the endogenous keratin IF network were visually assessed in transfected cells dual stained with antibodies to Myc and K8/K18. Cells displaying aberrant keratin IFs were subdivided into two categories: mildly abnormal cells exhibited an abnormal distribution of transfected protein but a normal looking endogenous keratin

network, and severely abnormal cells exhibited a disrupted endogenous filament network in addition to an aberrant distribution of the transfected protein.

Transient expression of Myc-wtK5 resulted in its incorporation into the endogenous keratin IF network without disruption (Figure 3, A–A″) in the majority of cells (~94%; Table 2). On the other hand, transfection of Myc-K5E477K, known to cause severe EBS disease (Stephens *et al.*, 1997; Pfendner *et al.*, 2003), resulted in altered keratin networks in 25.5% of transfected cells (Table 2), even though it was expressed at lower levels compared with wt K5 (Figure 1B). In 19.5% of Myc-K5E477K–transfected cells, the disruption included a marked collapse of the endogenous keratin IF network and was considered severe (Table 2; Figure 3, B–B″). By comparison, the milder EBS-causing Myc-K5-D328H mutant (Muller *et al.*, 1998) caused alterations with a frequency (11.4%) closer to that seen for wt K5, even though it was expressed at higher levels than Myc-K5-E477K (Figure 1B and Table 2). Only 7.6% of Myc-K5D328H–expressing mutant cells showed severely altered keratin networks (Table 2 and Figure 3, C–C″). Incorporating Myc-K5E477K and Myc-K5D328H in our analysis thus provided landmarks with which to assess the properties of K5 tail domain mutants.

The Myc-K5-1649delG protein exhibits one of two fates in transfected cells: integration within the endogenous network, generally with no or mild impact on its organization (Table 2), and formation of small aggregates in the perinu-

Table 2. Impact of mutant expression on keratin filament organization in transfected cells

	DNA construct transfected					
	wtK5	K5E477K	K5D328H	K5-1649delG	K5CΔ111	K5CΔ41
Transfection efficiency (%)	16.9	25.9	21.5	24.7	25.7	17.8
Abnormal cells (%)	6.2	25.5	11.4	16.6	17.9	14.0
Severe (%)	5.6	19.6	7.6	8.7	13.1	7.4
Mild (%)	0.6	5.9	3.8	7.9	4.8	6.6

For each DNA construct tested, >1000 cells were included as part of this analysis. Mildly abnormal refers to transfected cells in which the transfected protein exhibited an abnormal distribution but the endogenous keratin IF network seemed normal. Severely abnormal refers to transfected cells in which both the transfected protein and the endogenous keratin IF network exhibited a grossly abnormal distribution.
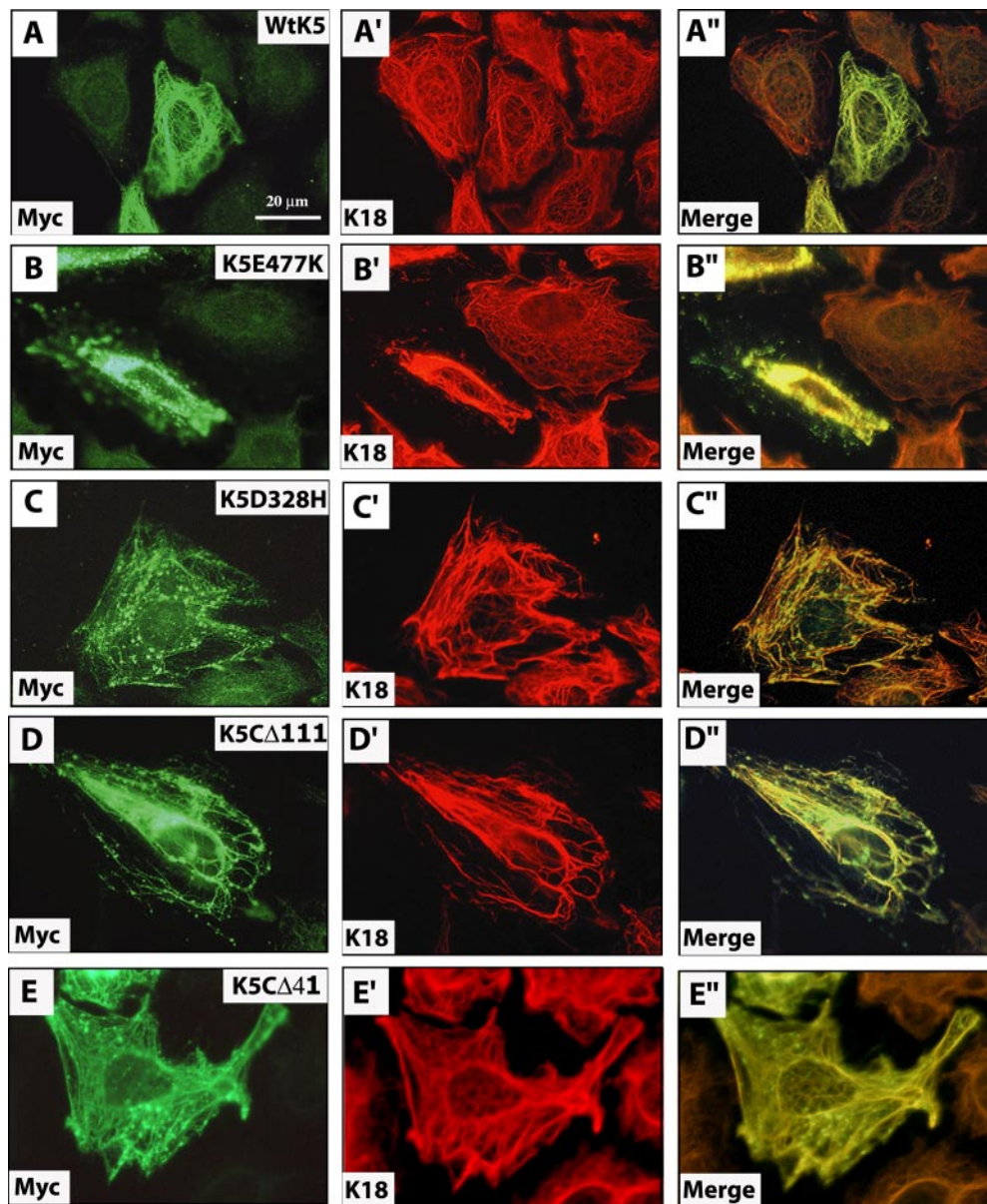
Figure 3. Impact of wild-type and mutant K5 expression on keratin filament organization in transfected cells. PtK2 kidney epithelial cells were transiently transfected with Myc-wtK5 (A–A″), Myc-K5E477K (B–B″), Myc-K5D328H (C–C″), Myc-K5CΔ111 (D–D″), or Myc-K5CΔ41 (E–E″) expression constructs. At 48 h posttransfection, cells were fixed and processed for double immunofluorescence staining by using antibodies to Myc, to detect the transfected protein, and K18, to visualize the endogenous keratin IF network. The identity of the labeled antigen is given in the lower left corner of each micrograph. See Table 2 for a quantitation of the outcome of these experiments.

clear cytoplasm (Figure 4, A–A″ and B—B″). The latter were seen in ~17% of transfected cells (Table 2). Although these Myc-positive aggregates were negative for endogenous keratin proteins, confocal microscopy confirmed that they were often apposed against keratin filaments in PtK2 cells (Figure 4, B–B″). Cotransfection of Myc-K5-1649delG and K14 resulted in their colocalization in the same model cell line (Figure 4, C–C″). Similar results were obtained when Myc-K5-1649delG was transiently expressed in mouse 308 epidermal keratinocytes (Figure 4, D–D″) which, like human epidermal keratinocytes in primary culture (Coulombe *et al.*, 1991), express K5, K6, K14, K16, and K17 as their main keratins (our unpublished data). By comparison, Myc-K5CΔ111 mutant protein caused endogenous keratin IFs to

bundle in ~13% of tranfected PtK2 cells and also was scattered in the form of fine aggregates in the cytoplasm (Figure 3, D–D″, and Table 2). Transient expression of Myc-K5CΔ41 mutant also gave rise to small aggregates in PtK2 cells, although their impact on the endogenous filament organization was milder (Figure 3, E–E″, and Table 2).

We subjected PtK2 cells expressing Myc-K5-1649delG or Myc-wtK5 to a detergent-based serial extraction to further analyze their properties. All of the detectable Myc-wtK5 and Myc-K5-1649delG occurred in the insoluble fraction, as seen for endogenous keratins (our unpublished data). These results suggest that the disruptive properties of the K5-1649delG mutant are intermediate between those of K5E477K and K5D328H, which cause severe and mild EBS
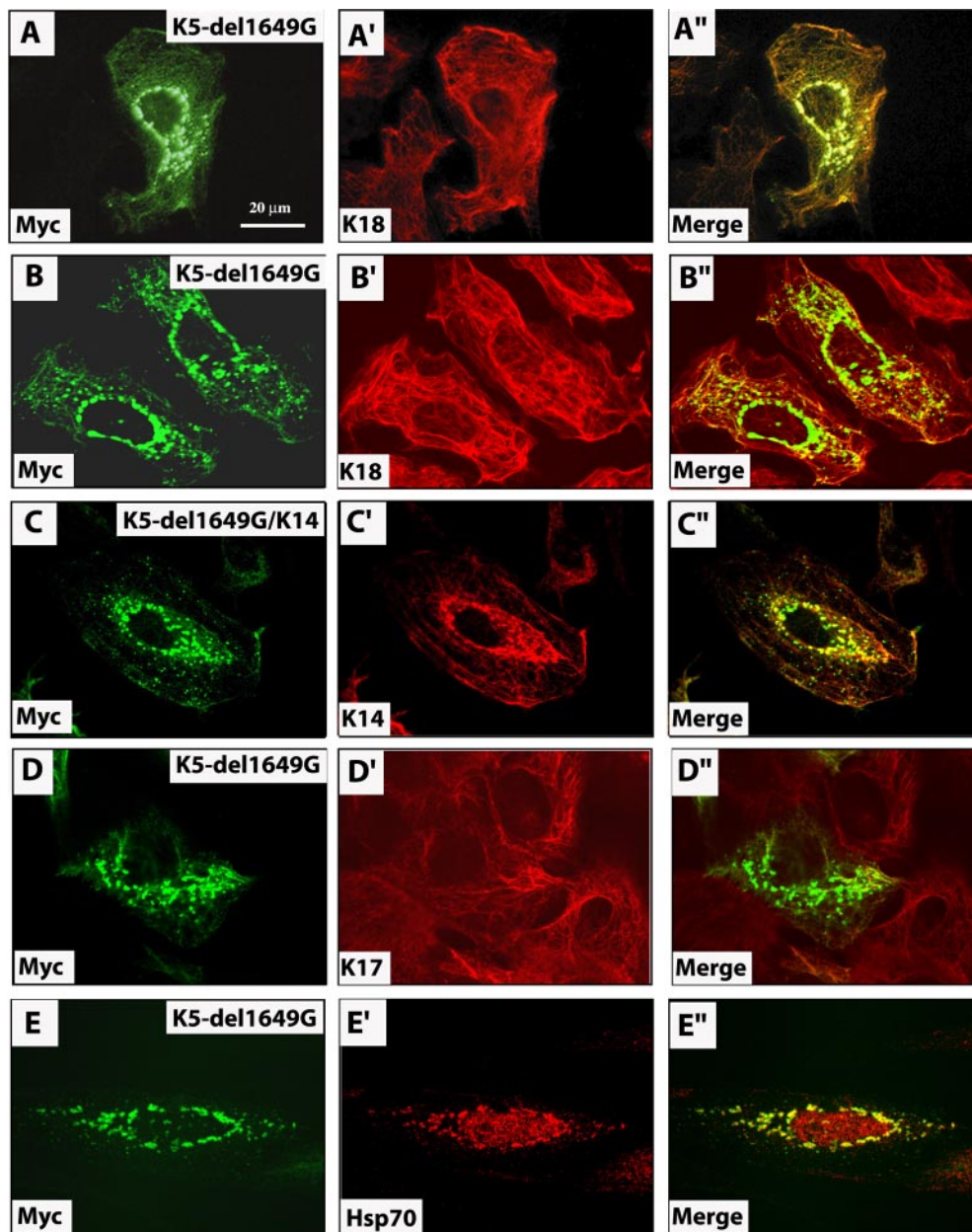
Figure 4. Impact of K5 tail domain mutant expression on keratin filament organization in transfected cells. PtK2 kidney epithelial cells (A, B, C, and E) or 308 mouse epidermal keratinocytes (D) were transiently transfected with Myc-K5-1649delG alone (A–A″, B–B″, D–D″, and E and E′) or along with K14 (C–C″). At 48 h posttransfection, cells were fixed and processed for double immunofluorescence staining by using antibodies to Myc, to detect the transfected protein, and K18, to visualize the endogenous keratin IF network (A–D), or hsp70 (E). The identity of the labeled antigen is given in the lower left corner of each micrograph. All micrographs except A–A″ were taken using a confocal microscope. See Table 2 for a quantitation of the outcome of these experiments.

disease, respectively, and extend the in vitro data in support of an important role for nonhelical tail domain of K5 toward the organization of keratin filaments in epithelial cells.

Studies Involving Isolated Tail Domains

Transiently expressed Myc-K5-1649delG mutant protein localizes to either filaments or aggregates, or both, raising the possibility of a competition between two distinct regions of the protein: the intact central α-helical rod domain, expected to direct the protein to filaments, and the mutated tail domain, which might interfere with this targeting and cause

the protein to form aggregates. To test this notion, DNA constructs were devised in which the tail domain of K5, wild-type, and 1649delG mutant were Myc epitope tagged at their N terminus. Transfected PtK2 cells were transiently transfected with Myc-T5 and Myc-T5-1649delG, prepared for double immunofluorescence, and analyzed by confocal microscopy. Myc-T5 exhibited a mixed pattern of localization in transfected cells, consisting of 1) diffuse distribution throughout the cytoplasm, 2) colocalization with cytoskeletal filaments, and 3) concentration as discrete patches at the cell periphery (Figure 5, A–A″). Examination of doubly
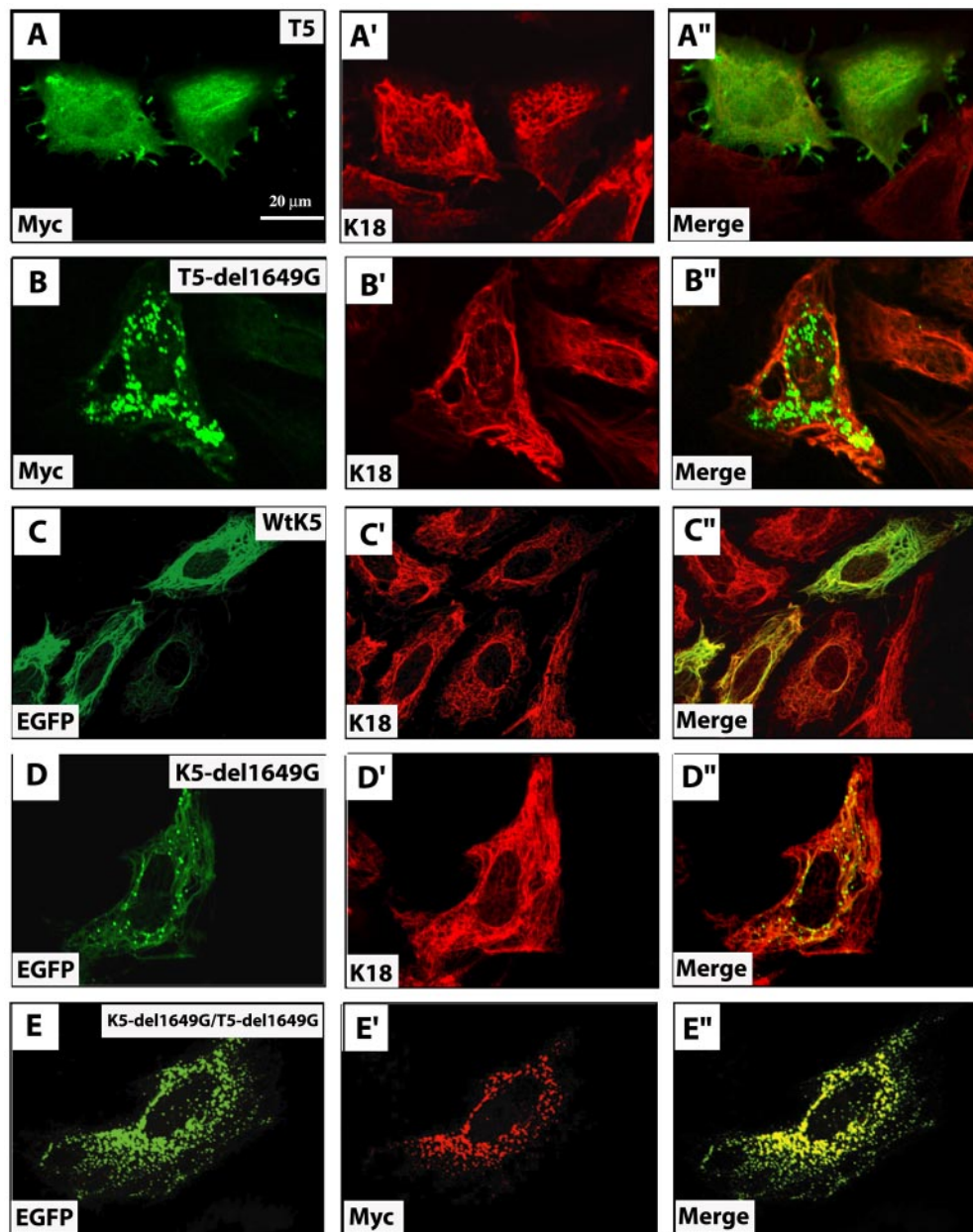
Figure 5. Fate of isolated K5 tail domain in transfected epithelial cells. PtK2 kidney epithelial cells were singly transfected with Myc-wtT5 (A–A″), Myc-T5-1649delG (B–B″), GFP-wtK5 (C–C″), GFP-K5-1649delG (D–D″), or doubly transfected with Myc-T5-1649delG and GFP-K5-1649delG (E–E″) expression constructs. At 48 h posttransfection, cells were fixed and processed for double immunofluorescence staining by using antibodies to Myc, to detect the transfected protein, and K18, to visualize the endogenous keratin IF network. GFP fusion proteins were detected using GFP-s intrinsic fluorescence. The identity of the labeled antigen is given in the lower left corner of each micrograph. See text for details.

stained preparations revealed that Myc-T5 was partially colocalized with endogenous K8/K18 filaments (Figure 5, A–A″). Transfected Myc-T5-1649delG protein was found exclusively in the form of aggregates throughout the cytoplasm, but with a predilection for the perinuclear region (Figure 5, B–B″). These aggregates were seen as early as 12 h posttransfection (our unpublished data). Again, many of these aggregates were apposed against endogenous keratin filaments, although their presence rarely affected their organization.

We next fused the enhanced green fluorescent protein (EGFP) coding sequence in-frame to the N terminus of full-length wtK5 and K5-1649delG. Transfection of EGFP-wtK5 resulted in its colocalization with endogenous keratin IFs in PtK2 cells (Figure 5, C–C″). Very few transfected cells showed disrupted IF networks (our unpublished data). Likewise, the behavior of transfected EGFP-K5-1649delG was virtually identical to Myc-K5-1649delG (Figure 5, D–D″). The availability of EGFP-K5-1649delG allowed us to test whether the mutated tail domain is directly responsible for the formation of cytoplasmic aggregates. We found that cotransfected EGFP-K5-1649delG and Myc-T5-1649delG were always part of the same aggregates (Figure 5, E–E″). The 1649delG mutation thus has very strong properties in that it

can prevent the rod domain from mediating the incorporation of the mutant protein into a preexisting keratin filament network.

Biochemical studies were conducted on K5 tail domain–transfected PtK2 cells. Sequential extraction followed by Western immunoblotting revealed a difference in the partitioning of Myc-T5 and Myc-T5-1649delG. Whereas all of the detectable Myc-T5-1649delG was retrieved in the final, insoluble protein fraction, ~50% of the Myc-T5 pool was found in the Triton X-100–soluble fraction and another ~15% was in the high-salt extract (Figure 6A). These results are consistent with the different distribution of each protein as seen by immunofluorescence (Figure 5). Next, we subjected transfected PtK2 cells to chemical cross-linking and then solubilized cells by Empigen BB, followed by immunoprecipitation with a K18 antibody. Both Myc-T5 and Myc-T5-1649delG were enriched in K18 immunoprecipitates, and comparatively little protein was precipitated in the nonimmune serum controls (Figure 6B). Omission of the cross-linking step gave rise to inconsistent results (our unpublished data). These results confirm and extend the morphological observation that both Myc-T5 and Myc-T5-1649delG are associated with K8/K18 filaments in transfected cells, albeit in a detergent-labile manner. Finally, we fused a His-tag at the N terminus of T5 to facilitate its recovery and purification after bacterial expression and to test whether its ability to associate with keratin IFs in transfected cells reflects a direct interaction. Unlike His-T14 (our unpublished data; see Bousquet *et al.*, 2001), however, purified His-T5 did not cosediment with K5/K14 IFs or vimentin IFs (Figure 6C).

Expression of K5-1649delG Does Not Elicit an Unfolded Protein Response

In many chronic diseases, the affected cells exhibit aggregates of mispolymerized and abnormally modified IF proteins (e.g., hyperphorphorylation, ubiquitination, and cleavage), eliciting an "unfolded protein response" (Zatloukal *et al.*, 2004). This can lead to cellular activation and release of cytokines. To investigate whether this is potentially the case in K5-1649delG–expressing cells, we sought to localize hsp70, hsp27, αB-crystallin, ubiquitin, and p62 in K5-1649delG–expressing PtK2 cells. All of these antigens are, along with K8/K18, components the Mallory Bodies that form in hepatocytes during several types of liver disease. Other than hsp70 (Figure 4, E–E′), which does bind K8-K18 under normal healthy conditions (Liao *et al.*, 1995), we find that K5-1649delG aggregates are negative for all these other antigens (our unpublished data).

DISCUSSION

Disease-based Evidence That the Nonhelical Tail Domain Influences Keratin Function In Vivo

A few instances of keratin tail domain mutations have now been shown to cause human disease. Thus, two dominantly acting, nonsense mutations affecting residues located at the extreme C terminus of the K5 rod domain (K472 and E477) give rise to EBS with generalized blistering (Muller *et al.*, 1999; Livingston *et al.*, 2001). Even though these C-terminal truncations occur only five residues apart within the highly conserved TYRK$_{472}$LLEGE$_{477}$ motif at the very end of the K5 rod domain, electron microscopy showed that only E477 is associated with keratin aggregates typical of Dowling–Meara EBS in basal cells. In yet another case involving K5's C terminus, a nucleotide deletion, 1635delG, was found
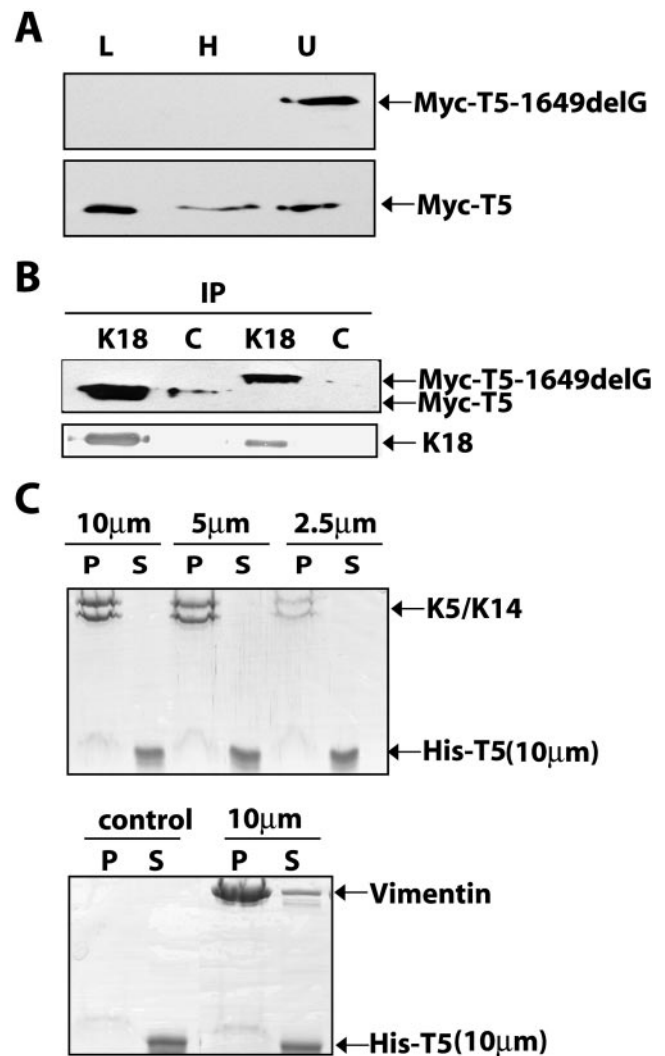

Figure 6. Biochemical and Immunological analyses of transfected proteins in PtK2 epithelial cells. (A) PtK2 kidney epithelial cells were transfected with Myc-wtT5 or Myc-T5-1649delG. At 48 h post-transfection, they were sequentially extracted to assess the distribution of transfected protein though SDS-PAGE and Western immunoblotting. Lanes are as follows: L, low-salt fraction; H, high-salt fraction; and U, final pellet solubilized in urea buffer. (B) PtK2 kidney epithelial cells were transfected with Myc-wtK5 or Myc-K5-1649delG, and 48 h later, were extracted with Empigen BB-containing buffer and subjected to immunoprecipitation by using rabbit immune serum to K18 or normal rabbit serum used as control (c). Immunoprecipitates were analyzed by Western blotting by using antibodies directed against Myc (top blot) and K18 (bottom blot. C) Cosedimentation assay in vitro. Reconstituted K5-K14 (10, 5, and 2.5 μm) or vimentin filaments (10 μm) were mixed with purified His-T5 (10 μm) and subjected to high-speed centrifugation (see *Materials and Methods*). Filaments were omitted in a tube acting as control. Pellet (P) and supernatant (S) fractions were analyzed by SDS-PAGE and Coomassie Blue staining.

within K5's exon 9 in a sporadic case of Weber–Cockayne (mild) EBS (Sprecher *et al.*, 2003). The resulting frameshift is in-phase with the K5-1649delG mutation, but the properties of this mutant have not been described. Three mutations affecting exon 9 in the K1 coding sequence (1609GG→A, 1628delG, and 1752insG) were linked to distinct clinical presentations, ichthyosis hystrix Curth–Macklin (a severe

and disfiguring condition apparent to EHK), striate palmo-plantar keratoderma, and mild epidermolytic hyperkeratosis (Sprecher *et al.*, 2001, 2003; Whittock *et al.*, 2002). K1 is expressed in the differentiating layers of interfollicular epidermis (O'Guin *et al.*, 1990; Fuchs, 1995). These frameshift-producing mutations contrast sharply with the missense alleles found in most instances of keratinopathies (Cassidy *et al.*, 2002). These findings underscore the importance of the nonhelical tail domain of keratins in vivo. Also of note, the C terminus of K18 is first subjected to caspase cleavage during apoptosis, perhaps reflecting the need to initially disrupt its function so that further cleavages can complete the breakdown of the keratin IF network during this process (Ku and Omary, 2001; Schutte *et al.*, 2004).

The tail domain is highly variable in length and primary structure among keratin proteins (Quinlan *et al.*, 1994), and its properties remain poorly understood. The short tail domain of K14 (~50 residues) behaves as a low-affinity keratin filament binding protein in vitro as well as in transfected cells and plays a role in the salt- and alkaline pH-induced bundling of K5/K14 filaments in vitro (Bousquet *et al.*, 2001). As shown here, such a direct interaction between the K5 tail domain and keratin filaments could not be evidenced using similar assays in vitro, although it occurs in transfected cells. Like other type II keratins found in epidermis, the tail domain of K5 features glycine loop motifs (Steinert *et al.*, 1991), which also occur in other epidermal structural proteins (loricrin and corneodesmosin) and in single-stranded RNA binding proteins (Steinert *et al.*, 1991). There is emerging evidence that glycine loops could mediate homophilic interactions (Jonca *et al.*, 2002; Caubet *et al.*, 2004). Clearly, additional studies are needed to identify the mechanism(s) that underlie the distribution of K5's tail domain in transfected cells.

A Keratin Mutation with Unusual Properties Is at the Source of an Atypical EBS Presentation

We show here that the C-terminal frameshift induced by a guanine nucleotide deletion, 1649delG, in the last exon of K5 affects the properties of the protein in a very unusual manner. In vitro, the structural features and micromechanical properties of K5-1649delG/K14 filaments are dramatically altered. Studies using the experimentally produced K5C∆41 suggest that the loss of the C-terminal 41 amino acid residues plays a role in determining the properties of K5-1649delG mutant protein. In transiently transfected kidney and skin epithelial cells in culture, the impact of K5-1649delG expression is not as disruptive and does not bear an obvious relationship to the in vitro findings. Thus, a fraction of the mutant protein incorporates into normal looking keratin IFs, whereas another fraction occurred in the form of small aggregates whose dispersion within the cytoplasm differed according to the cell line used. In any event, only a subset of transfected cells showing K5-1649delG–positive aggregates also have disrupted endogenous keratin IFs. Formation of small cytoplasmic aggregates seems to be an intrinsic property of the mutant tail domain, as shown by studies with T5-1649delG. The frequency with which the 1649delG mutation affects keratin IF organization in transfected cells is intermediate in severity compared with K5-E477K and K5D328H, two mutations that cause severe and mild EBS disease, respectively. In addition to underscoring the importance of assessing mutant keratin properties in various settings, these observations clearly indicate that the 1649delG mutation impacts K5's properties in more than one respect.

Our studies suggest that expression of the mutant K5-1649delG protein should lead to the fragilization of epidermal basal cells in vivo, the hallmark feature of EBS. They do not provide a basis for the observation of migratory erythema in the skin of these patients (Gu *et al.*, 2003), a very unusual phenomenon in the context of EBS (Fine *et al.*, 1991; Kawana *et al.*, 1994; Goldsmith, 2003). Database searching revealed that the novel stretch of 76 amino acids at the C terminus of K5-1649delG does not have a close relative in nature (our unpublished data). Although the K5-1649delG protein aggregates also contain hsp70 in transfected cells, perhaps reflecting a folding problem with its modified tail domain (Liao *et al.*, 1995), we could not find further evidence of elaboration of an unfolded protein response (Zatloukal *et al.*, 2004). This does not exclude the possibility that such a response, which may lead to the release of cytokines, could be elaborated in the patients' epidermis in vivo. Determining how K5-1649delG might elicit this odd phenomenon in patients' skin likely requires transgenic mouse work.

Live imaging studies of epithelial cell lines engineered to express a green fluorescent protein (GFP)-tagged version of K14 $Arg_{125}\rightarrow Cys$ showed that nascent mutant protein chains form small spherical aggregates at the cell periphery, which, unlike the corresponding wild-type protein, do not subsequently incorporate into keratin IFs (Werner *et al.*, 2004). These important findings provided a potential explanation for the specific location of the intracellular cleavage within epidermal basal cells in EBS, which invariably occurs between the nucleus and matrix-bound hemidesmosomes (Anton-Lamprecht, 1983). The possibility that disease-causing mutant proteins could interfere with the dynamics of IFs under steady-state conditions in vivo is worth pursuing further. Because of their distinct intracellular distribution, it seems unlikely that the small aggregates containing K5-1649delG in transfected cells correspond to the "normal" keratin filament precursors seen by Windoffer *et al.* (2004) in their live imaging studies.

Pathogenesis of Blister Formation in EBS: Is There More to It than Defective Cellular Mechanics?

The genetic basis of EBS was discovered more than a dozen years ago (Bonifas *et al.*, 1991; Coulombe *et al.*, 1991; Lane *et al.*, 1992). Along with studies involving mouse models, the large number of mutations in the K5 and K14 coding sequences uncovered since then (~140; Cassidy *et al.*, 2002) laid the foundation for a good, albeit superficial, understanding of genotype–phenotype correlations in EBS (Fuchs and Cleveland, 1998; Irvine and McLean, 1999; Omary *et al.*, 2004). Indeed, the subcellular mechanism(s) underlying blister formation in EBS and other keratin-based disorders remains incompletely understood. Cell fragility is clearly involved, as supported by several lines of evidence (Fuchs and Cleveland, 1998; Omary *et al.*, 2004). There are, however, some hints that mechanism(s) other than mechanical failure also contribute to disease pathogenesis in EBS and related disorders. This may be especially true in circumstances in which the disease-causing mutant protein triggers the formation of abnormal aggregates in the cytoplasm (Omary *et al.*, 2004; Zatloukal *et al.*, 2004).

The presence of mutant keratin-containing aggregates could place epithelial cells under metabolic stress or alter its response to proapoptotic signals. Keratinocyte cell lines established from EBS patients show an earlier activation of cellular kinases, including the stress response-related c-Jun NH_2-terminal kinase, than control cells after an osmotic shock (D'Alessandro *et al.*, 2002). In another study, Yoneda *et al.* (2004) reported that stable expression of K14 $Arg_{125}\rightarrow Cys$

in HaCaT keratinocytes leads to enhanced secretion of tumor necrosis factor (TNF)-α. This mutant also was found to abrogate the ability of K14 to interact with TRADD, an adaptor molecule essential for the apoptotic response that may ensue engagement of TNF-R1. These authors speculated that such changes could lead to cellular death by apoptosis in the epidermis of EBS patients harboring the K14 $Arg_{125}\rightarrow Cys$. Intriguingly, there are EBS-causing mutations that inactive the functional caspase cleavage motif in the middle linker region (L12) within the rod domain of K14 and related type I keratins (Ku and Omary, 2001). There has been no report of apoptosis-like nuclear condensation in basal keratinocytes in the skin of EBS patients. Although we await the evidence supporting that cellular stress and/or apoptosis do contribute to disease pathogenesis in vivo, such newly postulated mechanisms could explain the atypical spreading of skin lesions as is seen in EBS-MCE.

ACKNOWLEDGMENTS

REFERENCES

Albers, K., and Fuchs, E. (1987). The expression of mutant epidermal keratin cDNAs transfected in simple epithelial and squamous cell carcinoma lines. J. Cell Biol. 105, 791–806.

Anton-Lamprecht, I. (1983). Genetically induced abnormalities of epidermal differentiation and ultrastructure in ichthyoses and epidermolyses: pathogenesis, heterogeneity, fetal manifestation, and prenatal diagnosis. J. Investig. Dermatol 81, 149s–156s.

Bonifas, J. M., Rothman, A. L., Epstein, E. H., Jr. (1991). Epidermolysis bullosa simplex: evidence in two families for keratin gene abnormalities. Science 254, 1202–1205.

Bousquet, O., Ma, L., Yamada, S., Gu, C., Idei, T., Takahashi, K., Wirtz, D., and Coulombe, P. A. (2001). The nonhelical tail domain of keratin 14 promotes filament bundling and enhances the mechanical properties of keratin intermediate filaments in vitro. J. Cell Biol. 155, 747–754.

Boussif, O., Lezoualc'h, F., Zanta, M. A., Mergny, M. D., Scherman, D., Demeneix, B., and Behr, J. P. (1995). A versatile vector for gene and oligonucleotide transfer into cells in culture and in vivo: polyethylenimine. Proc. Natl. Acad. Sci. USA 92, 7297–7301.

Cassidy, A. J., Lane, E. B., and McLean, W.H.I. (2002). The human intermediate filament mutation database. Available at: http://www.interfil.org. Accessed on January 27, 2005.

Caubet, C., Jonca, N., Lopez, F., Esteve, J. P., Simon, M., and Serre, G. (2004). Homo-oligomerization of human corneodesmosin is mediated by its N-terminal glycine loop domain. J. Investig. Dermatol. 122, 747–754.

Chavanas, S., Pulkkinen, L., Gache, Y., Smith, F. J., McLean, W. H., Uitto, J., Ortonne, J. P., and Meneguzzi, G. (1996). A homozygous nonsense mutation in the PLEC1 gene in patients with epidermolysis bullosa simplex with muscular dystrophy. J. Clin. Investig. 98, 2196–2200.

Chavez Zobel, A. T., Loranger, A., Marceau, N., Theriault, J. R., Lambert, H., and Landry, J. (2003). Distinct chaperone mechanisms can delay the formation of aggresomes by the myopathy-causing R120G alphaB-crystallin mutant. Hum. Mol. Genet. 12, 1609–1620.

Chou, C. F., Riopel, C. L., Rott, L. S., and Omary, M. B. (1993). A significant soluble keratin fraction in "simple" epithelial cells. Lack of an apparent phosphorylation and glycosylation role in keratin solubility. J. Cell Sci. 105, 433–445.

Coulombe, P. A., Bousquet, O., Ma, L., Yamada, S., and Wirtz, D. (2000). The 'ins' and 'outs' of intermediate filament organization. Trends Cell Biol. 10, 420–428.

Coulombe, P. A., and Fuchs, E. (1990). Elucidating the early stages of keratin filament assembly. J. Cell Biol. 111, 153–169.

Coulombe, P. A., Hutton, M. E., Letai, A., Hebert, A., Paller, A. S., and Fuchs, E. (1991). Point mutations in human keratin 14 genes of epidermolysis bullosa simplex patients: genetic and functional analyses. Cell 66, 1301–1311.

Coulombe, P. A., Ma, L., Yamada, S., and Wawersik, M. (2001). Intermediate filaments at a glance. J. Cell Sci. 114, 4345–4347.

Coulombe, P. A., Tong, X., Mazzalupo, S., Wang, Z., and Wong, P. (2004). Great promises yet to be fulfilled: defining keratin intermediate filament function in vivo. Eur. J. Cell Biol. 83, 735–746.

D'Alessandro, M., Russell, D., Morley, S. M., Davies, A. M., and Lane, E. B. (2002). Keratin mutations of epidermolysis bullosa simplex alter the kinetics of stress response to osmotic shock. J. Cell Sci. 115, 4341–4351.

Ferry, J. (1980). Viscoelastic Properties of Polymers, New York: John Wiley & Sons.

Fine, J. D., et al. (1991). Revised clinical and laboratory criteria for subtypes of inherited epidermolysis bullosa. A consensus report by the Subcommittee on Diagnosis and Classification of the National Epidermolysis Bullosa Registry. J. Am. Acad. Dermatol. 24, 119–135.

Fontao, L., Tasanen, K., Huber, M., Hohl, D., Koster, J., Bruckner-Tuderman, L., Sonnenberg, A., and Borradori, L. (2004). Molecular consequences of deletion of the cytoplasmic domain of bullous pemphigoid 180 in a patient with predominant features of epidermolysis bullosa simplex. J. Investig. Dermatol. 122, 65–72.

Franke, W. W., Schmid, E., Osborn, M., and Weber, K. (1978). Different intermediate-sized filaments distinguished by immunofluorescence microscopy. Proc. Natl. Acad. Sci. USA 75, 5034–5038.

Fuchs, E. (1995). Keratins and the skin. Annu. Rev. Cell Dev. Biol. 11, 123–153.

Fuchs, E., and Cleveland, D. W. (1998). A structural scaffolding of intermediate filaments in health and disease. Science 279, 514–519.

Goldsmith, L. A. (2003). Migrating skin lesions: a genetic clue. J. Investig. Dermatol. 121, vii-viii.

Gu, L. H., Kim, S. C., Ichiki, Y., Park, J., Nagai, M., and Kitajima, Y. (2003). A usual frameshift and delayed termination codon mutation in keratin 5 causes a novel type of epidermolysis bullosa simplex with migratory circinate erythema. J. Investig. Dermatol. 121, 482–485.

Herrmann, H., and Aebi, U. (2004). Intermediate filaments: molecular structure, assembly mechanism, and integration into functionally distinct intracellular scaffolds. Annu. Rev. Biochem. 73, 749–789.

Herrmann, H., Hesse, M., Reichenzeller, M., Aebi, U., and Magin, T. M. (2003). Functional complexity of intermediate filament cytoskeletons: from structure to assembly to gene ablation. Int. Rev. Cytol. 223, 83–175.

Hesse, M., Magin, T. M., and Weber, K. (2001). Genes for intermediate filament proteins and the draft sequence of the human genome: novel keratin genes and a surprisingly high number of pseudogenes related to keratin genes 8 and 18. J. Cell Sci. 114, 2569–2575.

Huber, M., Florth, M., Borradori, L., Schacke, H., Rugg, E. L., Lane, E. B., Frenk, E., Hohl, D., and Bruckner-Tuderman, L. (2002). Deletion of the cytoplasmatic domain of BP180/collagen XVII causes a phenotype with predominant features of epidermolysis bullosa simplex. J. Investig. Dermatol. 118, 185–192.

Irvine, A. D., McKenna, K. E., Jenkinson, H., and Hughes, A. E. (1997). A mutation in the V1 domain of keratin 5 causes epidermolysis bullosa simplex with mottled pigmentation. J. Investig. Dermatol. 108, 809–810.

Irvine, A. D., and McLean, W. H. (1999). Human keratin diseases: the increasing spectrum of disease and subtlety of the phenotype-genotype correlation. Br. J. Dermatol. 140, 815–828.

Jonca, N., Guerrin, M., Hadjiolova, K., Caubet, C., Gallinaro, H., Simon, M., and Serre, G. (2002). Corneodesmosin, a component of epidermal corneocyte desmosomes, displays homophilic adhesive properties. J. Biol. Chem. 277, 5024–5029.

Jonkman, M. F., Pas, H. H., Nijenhuis, M., Kloosterhuis, G., and Steege, G. (2002). Deletion of a cytoplasmic domain of integrin beta4 causes epidermolysis bullosa simplex. J. Investig. Dermatol. 119, 1275–1281.

Kawana, S., Hashimoto, I., and Nishiyama, S. (1994). Epidermolysis bullosa simplex with transient erythema circinatum. Br. J. Dermatol. 131, 571–576.

Kitajima, Y., Inoue, S., and Yaoita, H. (1989). Abnormal organization of keratin intermediate filaments in cultured keratinocytes of epidermolysis bullosa simplex. Arch. Dermatol. Res. 281, 5–10.

Ku, N. O., and Omary, M. B. (2001). Effect of mutation and phosphorylation of type I keratins on their caspase-mediated degradation. J. Biol. Chem. 276, 26792–26798.

Lane, E. B., Rugg, E. L., Navsaria, H., Leigh, I. M., Heagerty, A. H., Ishida, Y. A., and Eady, R. A. (1992). A mutation in the conserved helix termination peptide of keratin 5 in hereditary skin blistering. Nature 356, 244–246.

Lersch, R., Stellmach, V., Stocks, C., Giudice, G., and Fuchs, E. (1989). Isolation, sequence, and expression of a human keratin K5 gene: transcriptional regulation of keratins and insights into pairwise control. Mol. Cell. Biol. 9, 3685–3697.

Letai, A., Coulombe, P. A., McCormick, M. B., Yu, Q. C., Hutton, E., and Fuchs, E. (1993). Disease severity correlates with position of keratin point mutations in patients with epidermolysis bullosa simplex. Proc. Natl. Acad. Sci. USA 90, 3197–3201.

Liao, J., Lowthert, L. A., Ghori, N., and Omary, M. B. (1995). The 70-kDa heat shock proteins associate with glandular intermediate filaments in an ATP-dependent manner. J. Biol. Chem. 270, 915–922.

Livingston, R. J., Sybert, V. P., Smith, L. T., Dale, B. A., Presland, R. B., and Stephens, K. (2001). Expression of a truncated keratin 5 may contribute to severe palmar–plantar hyperkeratosis in epidermolysis bullosa simplex patients. J. Investig. Dermatol. 116, 970–974.

Ma, L., Yamada, S., Wirtz, D., and Coulombe, P. A. (2001). A 'hot-spot' mutation alters the mechanical properties of keratin filament networks. Nat. Cell Biol. 3, 503–506.

Moll, R., Franke, W. W., Schiller, D. L., Geiger, B., and Krepler, R. (1982). The catalog of human cytokeratins: patterns of expression in normal epithelia, tumors and cultured cells. Cell 31, 11–24.

Muller, F. B., Anton-Lamprecht, I., Kuster, W., and Korge, B. P. (1999). A premature stop codon mutation in the 2B helix termination peptide of keratin 5 in a German epidermolysis bullosa simplex Dowling-Meara case. J. Investig. Dermatol. 112, 988–990.

Muller, F. B., Kuster, W., Bruckner-Tuderman, L., and Korge, B. P. (1998). Novel K5 and K14 mutations in German patients with the Weber-Cockayne variant of epidermolysis bullosa simplex. J. Investig. Dermatol. 111, 900–902.

O'Guin, W. M., Schermer, A., Lynch, M., and Sun, T.-T. (1990). Differentiation-specific expression of keratin pairs. In: Cellular and Molecular Biology of Intermediate Filaments, ed. R. D. Goldman and P. M. Steinert, New York: Plenum Press, 301–334.

Omary, M. B., Coulombe, P. A., and McLean, W.H.I. (2004). Intermediate filaments and their associated diseases. N. Engl. J. Med. 351, 2087–2100.

Paller, A. S. (2004). The complexities of epidermolysis bullosa "simplex". J. Investig. Dermatol. 122, vi-vii.

Pfendner, E. G., Nakano, A., Pulkkinen, L., Christiano, A. M., and Uitto, J. (2003). Prenatal diagnosis for epidermolysis bullosa: a study of 144 consecutive pregnancies at risk. Prenat. Diagn. 23, 447–456.

Porter, R. M., and Lane, E. B. (2003). Phenotypes, genotypes and their contribution to understanding keratin function. Trends Genet 19, 278–285.

Pulkkinen, L., Smith, F. J., Shimizu, H., Murata, S., Yaoita, H., Hachisuka, H., Nishikawa, T., McLean, W. H., and Uitto, J. (1996). Homozygous deletion mutations in the plectin gene (PLEC1) in patients with epidermolysis bullosa simplex associated with late-onset muscular dystrophy. Hum. Mol. Genet. 5, 1539–1546.

Purkis, P. E., Steel, J. B., Mackenzie, I. C., Nathrath, W. B., Leigh, I. M., and Lane, E. B. (1990). Antibody markers of basal cells in complex epithelia. J. Cell Sci. 97, 39–50.

Quinlan, R., Hutchinson, C., and Lane, B. (1994). Intermediate filament proteins. Protein Profile 1, 779–911.

Schutte, B., et al. (2004). Keratin 8/18 breakdown and reorganization during apoptosis. Exp. Cell Res. 297, 11–26.

Smith, F. J., et al. (1996). Plectin deficiency results in muscular dystrophy with epidermolysis bullosa. Nat. Genet. 13, 450–457.

Sprecher, E., Ishida-Yamamoto, A., Becker, O. M., Marekov, L., Miller, C. J., Steinert, P. M., Neldner, K., and Richard, G. (2001). Evidence for novel functions of the keratin tail emerging from a mutation causing ichthyosis hystrix. J. Investig. Dermatol. 116, 511–519.

Sprecher, E., Yosipovitch, G., Bergman, R., Ciubutaro, D., Indelman, M., Pfendner, E., Goh, L. C., Miller, C. J., Uitto, J., and Richard, G. (2003). Epidermolytic hyperkeratosis and epidermolysis bullosa simplex caused by frameshift mutations altering the v2 tail domains of keratin 1 and keratin 5. J. Investig. Dermatol. 120, 623–626.

Steinert, P. M., Mack, J. W., Korge, B. P., Gan, S. Q., Haynes, S. R., and Steven, A. C. (1991). Glycine loops in proteins: their occurrence in certain intermediate filament chains, loricrins and single-stranded RNA binding proteins. Int. J. Biol. Macromol. 13, 130–139.

Stephens, K., Ehrlich, P., Weaver, M., Le, R., Spencer, A., and Sybert, V. P. (1997). Primers for exon-specific amplification of the KRT5 gene: identification of novel and recurrent mutations in epidermolysis bullosa simplex patients. J. Investig. Dermatol. 108, 349–353.

Strickland, J. E., Greenhalgh, D. A., Koceva-Chyla, A., Hennings, H., Restrepo, C., Balaschak, M., and Yuspa, S. H. (1988). Development of murine epidermal cell lines which contain an activated rasHa oncogene and form papillomas in skin grafts on athymic nude mouse hosts. Cancer Res. 48, 165–169.

Uttam, J., Hutton, E., Coulombe, P. A., Anton-Lamprecht, I., Yu, Q. C., Gedde-Dahl, T., Jr., Fine, J. D., and Fuchs, E. (1996). The genetic basis of epidermolysis bullosa simplex with mottled pigmentation. Proc. Natl. Acad. Sci. USA 93, 9079–9084.

Wawersik, M., Paladini, R. D., Noensie, E., and Coulombe, P. A. (1997). A proline residue in the alpha-helical rod domain of type I keratin 16 destabilizes keratin heterotetramers and influences incorporation into filaments. J. Biol. Chem. 272, 32557–32565.

Werner, N. S., Windoffer, R., Strnad, P., Grund, C., Leube, R. E., and Magin, T. M. (2004). Epidermolysis bullosa simplex-type mutations alter the dynamics of the keratin cytoskeleton and reveal a contribution of actin to the transport of keratin subunits. Mol. Biol. Cell 15, 990–1002.

Whittock, N. V., Smith, F. J., Wan, H., Mallipeddi, R., Griffiths, W. A., Dopping-Hepenstal, P., Ashton, G. H., Eady, R. A., McLean, W. H., and McGrath, J. A. (2002). Frameshift mutation in the V2 domain of human keratin 1 results in striate palmoplantar keratoderma. J. Investig. Dermatol. 118, 838–844.

Wilson, A. K., Coulombe, P. A., and Fuchs, E. (1992). The roles of K5 and K14 head, tail, and R/K L L E G E domains in keratin filament assembly in vitro. J. Cell Biol. 119, 401–414.

Windoffer, R., Woll, S., Strnad, P., and Leube, R .E. (2004). Identification of novel principles of keratin filament network turnover in living cells. Mol. Biol. Cell 15, 2436–2448.

Wong, P., and Coulombe, P. A. (2003). Loss of keratin 6 (K6) proteins reveals a function for intermediate filaments during wound repair. J. Cell Biol. 163, 327–337.

Wong, P., Domergue, R., and Coulombe, P. A. (2005). Overcoming functional redundancy to elicit pachyonychia congenita-like nail lesions in transgenic mice. Mol. Cell. Biol. 25, 197–205.

Worman, H. J., and Courvalin, J. C. (2004). How do mutations in lamins A and C cause disease? J. Clin. Investig. 113, 349–351.

Yamada, S., Wirtz, D., and Coulombe, P. A. (2002). Pairwise assembly determines the intrinsic potential for self-organization and mechanical properties of keratin filaments. Mol. Biol. Cell 13, 382–391.

Yamada, S., Wirtz, D., and Coulombe, P. A. (2003). The mechanical properties of simple epithelial keratins 8 and 18, discriminating between interfacial and bulk elasticities. J. Struct. Biol. 143, 45–55.

Yoneda, K., Furukawa, T., Zheng, Y. J., Momoi, T., Izawa, I., Inagaki, M., Manabe, M., and Inagaki, N. (2004). An autocrine/paracrine loop linking keratin 14 aggregates to tumor necrosis factor α-mediated cytotoxicity in a keratinocyte model of epidermolysis bullosa simplex. J. Biol. Chem. 279, 7296–7303.

Zatloukal, K., Stumptner, C., Fuchsbichler, A., Fickert, P., Lackner, C., Trauner, M., and Denk, H. (2004). The keratin cytoskeleton in liver diseases. J. Pathol. 204, 367–376.